

Crown-CAM: Reliable Visual Explanations for Tree Crown Detection in Aerial Images

Seyed Mojtaba Marvasti-Zadeh, *Member, IEEE*, Devin Goodman, Nilanjan Ray, *Member, IEEE*, Nadir Erbilgin

Abstract—Visual explanation of “black-box” models has enabled researchers and experts in *artificial intelligence* (AI) to exploit the localization abilities of such methods to a much greater extent. Despite most of the developed visual explanation methods applied to single object classification problems, they are not well-explored in the detection task, where the challenges may go beyond simple coarse area-based discrimination. This is of particular importance when a detector should face several objects with different scales from various viewpoints or if the objects of interest are absent. In this paper, we propose Crown-CAM to generate reliable visual explanations for the challenging and dynamic problem of tree crown detection in aerial images. It efficiently provides fine-grain localization of tree crowns and non-contextual background suppression for scenarios with highly dense forest trees in the presence of potential distractors or scenes without tree crowns. Additionally, two *Intersection over Union* (IoU)-based metrics are introduced that can effectively quantify both the accuracy and inaccuracy of generated visual explanations with respect to regions with or without tree crowns in the image. Empirical evaluations demonstrate that the proposed Crown-CAM outperforms the Score-CAM, Augmented Score-CAM, and Eigen-CAM methods by an average IoU margin of 8.7, 5.3, and 21.7 (and 3.3, 9.8, and 16.5) respectively in improving the accuracy (and decreasing inaccuracy) of visual explanations on the challenging NEON tree crown dataset.

Index Terms—Explainable artificial intelligence (XAI), Tree crown detection, Class activation map (CAM), Interpretable deep learning.

I. INTRODUCTION

EXPLAINABLE *artificial intelligence* (XAI) consists of methods that allow humans to describe, interpret, and understand the predictions of “black-box” models (e.g., deep learning) to ensure end-users can trust the model to provide accurate decisions. In general, XAI methods can be classified based on their interpretability (e.g., perceptive or mathematical structures), methodology (e.g., gradient-based or gradient-free), and model usage (e.g., model-specific or post-hoc) [1], [2]. A widely-adopted approach of these methods is *class activation mapping* (CAM) to generate a saliency map (or heat-maps) highlighting which features of a given input significantly affect on the final decision of the model. Meanwhile, among XAI methods, post-hoc perceptive gradient-free methods are of interest due to their advantages, such as being model-agnostic without sacrificing trained model

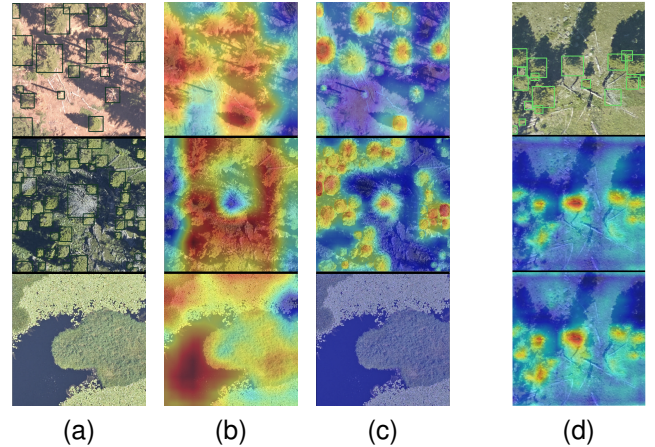


Fig. 1. Comparison of (a-c): CAMs generated for various scenarios of tree crown detection and (d): impact of removing redundant activation maps. Here, (a) illustrates the detected crowns by DeepForest model [3], (b) shows the CAMs by Score-CAM [4], (c) presents the CAMs generated by proposed Crown-CAM, and (d) shows the detected tree crowns (top row) and CAMs generated from all (middle row) and a half (bottom row) of the activation maps. Our Crown-CAM addresses the coarse localization problem of Score-CAM (e.g., top two rows of (c)) while suppressing background channels of CAMs (e.g., bottom row of (c)).

accuracy, applicable to models with non-differentiable outputs, and compatible with human perception.

While the demand for interpretability of deployed AI models via the XAI framework is becoming an unavoidable task in computer vision, explainability remains an emerging concept in solving some complex problems. Tree crown detection is one of these challenging problems in forest remote sensing. It is the critical first step that enables ecologists, foresters, biologists, and land managers to perform tasks such as monitoring vegetation changes, detecting insect infestations, estimating tree density, and identifying tree species. However, the usage of XAI methods in detecting tree crowns has not been investigated despite their wide application for generic object classification. Further, in contrast to XAI applications in classification that mainly involves a few large objects, tree crown detectors involve challenging scenarios, including dense forests with highly overlapping tree crowns, small tree crowns, and potential distractors. Despite the overlap between the generated CAM and the estimated bounding boxes, the visual explanations can provide beyond contextual information to refine noisy predictions further or support in-depth analysis of the overall process. Based on these motivations, this work aims to provide reliable visual explanations and relevant quantitative evaluation metrics for tree crown detection in aerial images.

This work is motivated by the simple yet effective Score-

S.M. Marvasti-Zadeh and N. Erbilgin are with the Department of Renewable Resources, University of Alberta, Canada ({mojtaba.marvasti, erbilgin}@ualberta.ca), D. Goodman is with the Canadian Forest Service, Natural Resources Canada, Canada (devin.goodman@nrcan-rncan.gc.ca), and N. Ray is with the Department of Computing Science, University of Alberta, Canada (nray1@ualberta.ca).

Manuscript received...; revised...

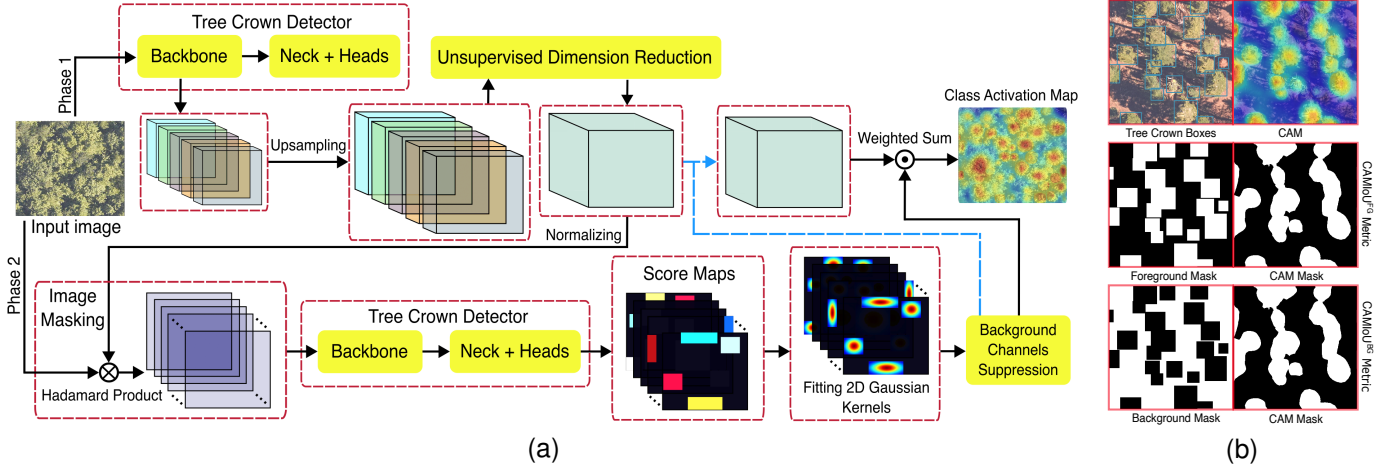


Fig. 2. An overview of (a) proposed Crown-CAM and (b) generated masks for introduced IoU-based localization metrics. (a) In the first phase, an input image is fed into a well-trained detector to extract the activation of backbone layers, tree crown bounding boxes, and their confidence scores. Next, the proposed unsupervised dimension reduction is used to retain information-rich activation maps and discard redundant ones. In the second phase, the input image is masked by the normalized selected activation maps, and then the masked images are passed into the tree crown detector to calculate local score maps. Further, local score maps are fitted with 2D Gaussian kernels to avoid boundary effects. Following that, the score map channels corresponding to the background are suppressed and excluded from the selected activation maps (blue dash arrow). Finally, the weighted sum of Gaussian fitted score maps and selected activation maps generate the tree crown CAM. (b) Based on the generated CAM and the bounding boxes of tree crowns, three masks are generated to calculate the localization accuracy (i.e., overlap with tree crowns) and inaccuracy (i.e., overlap with background regions) of visual explanations.

CAM method [4], which generates CAMs with promising accuracy and robustness that is independent of gradient computation. It uses (normalized and upsampled) convolutional activation maps as masks on the input image and then passes them to the network to compute one score for each activation map. At last, CAM for a class is generated by the weighted sum of activation maps using normalized scores. The Score-CAM has the main disadvantage of coarse localization of generated CAMs [5], [6] which prevents it from performing well in detecting tree crowns from aerial views (see Fig. 1b). Several extensions of Score-CAM have been proposed to obtain more accurate and visually sharper CAMs; however, these methods significantly increase computational complexity by combining Score-CAM's pipeline with additional operations or iterations. For instance, the SS-CAM [5], IS-CAM [6], and Augmented Score-CAM [7], respectively, utilize smooth operation, integration operation, and augmented activation maps to reduce inaccurate localization or capture more parts of an object. Meanwhile, the effectiveness of these methods has been evaluated based on qualitative metrics that are both designed for the classification task and focus solely on the objects within a scene. However, these metrics lack the ability to assess the localization accuracy of CAMs in detecting objects and fail to recognize the overlap (or the inaccuracy) between the generated CAMs and the background pixels (e.g., when there is no object in a scene). In contrast, we propose Crown-CAM, which provides reliable CAMs for tree crown detection models without considerably increasing the computational burden (see Fig. 1c). Moreover, inspired by *weakly-supervised localization* (WSL) of CAMs (e.g., [8]), two metrics are introduced that efficiently quantify the accuracy & inaccuracy of visual explanations with respect to the tree crowns and background regions. In the WSL, the IoU metric is calculated between the ground-truth bounding box and a bounding box drawn around

the single largest segment of binarized CAM. However, we overcome its limitations by extending this metric to the tree crown detection task involving multiple targets with varying confidence scores and efficiently calculating the IoU between a collection of tree crown bounding boxes and a segmented CAM. We also propose an additional metric that calculates the inaccuracy of CAMs when they drift into background regions or are generated in the absence of tree crowns.

In summary, the main contributions are as follows.

- Our proposed Crown-CAM makes it possible to generate reliable CAMs for detecting tree crowns.
- We propose unsupervised dimension reduction of activation maps to provide computational efficiency by excluding redundant activation maps and emphasizing informative ones (see Fig. 1d).
- The proposed Crown-CAM computes local score maps rather than one global score per activation map used in prior efforts. Hence, area-based scores merely enable target-related areas of activation maps to provide more accurate CAMs for challenging detection scenarios. In addition, 2D Gaussian kernels are fitted to tree crown areas to reduce the boundary effects of local scores.
- We propose a background channel suppression strategy based on the calculated score maps to avoid misleading activation maps that do not locate the tree crowns.
- Two useful IoU-based metrics are introduced that quantify the accuracy (and inaccuracy) of the generated CAM in comparison with dense tree crowns (or background areas).

The rest of the paper is organized as follows. The proposed Crown-CAM and localization metrics are described in detail in Section II and Section III. In Section IV, empirical evaluations and comparisons are presented. Finally, the conclusion is summarized in Section V.

II. PROPOSED METHOD: CROWN-CAM

In this section, we introduce Crown-CAM, which enables explanation visualization of tree crown detectors in challenging aerial scenarios. An overview of the proposed method is presented in Fig. 2a. The Crown-CAM comprises two main phases: i) extracting activation maps from all backbone layers of a tree crown detector (and tree crown bounding boxes & their confidence scores), and unsupervised dimension reduction, and ii) image masking, local score map calculation, fitting 2D Gaussian kernels to the score maps, and background channels suppression. A pseudo-code for our Crown-CAM is shown in Algorithm 1. Each step is described in detail in the following subsections.

A. Phase 1: Unsupervised Selection of Activation Maps

In this phase, we seek to minimize the computational complexity of high-dimensional activation maps required to generate CAMs for the detection task (in contrast to previous cumbersome classification methods requiring extra operations and iterations [5]–[7]). For a given input image $X \in \mathbb{R}^{3 \times w \times h}$ (w and h refer to width and height), we can use a well-trained tree crown detector f to extract activation maps \mathbb{A} from backbone layers $l \in [1, \dots, L]$ (each having C channels) in addition to detected bounding boxes B^X and corresponding confidence scores Y^X . When using XAI for classification tasks, a widely-adopted technique is to extract activation maps only from the last backbone layer, thus reducing the computational burden. However, the spatial resolution of these activation maps is too coarse to generate accurate CAMs for challenging tree crown detection scenarios, requiring pixel-accurate localization. Hence, the Crown-CAM involves the activation maps of all backbone layers to generate reliable CAMs that incorporate fine-grained tree crown information.

Next, the extracted activation maps are upsampled (i.e., $\mathbb{U} \in \mathbb{R}^{(L \times C) \times w \times h}$) by applying bi-linear interpolation to match the input image size. The baseline Score-CAM [4] (and its extensions [5]–[7]) perturbs an input image with these activation maps and calculates their importance. However, not all of the extracted activation maps contribute significantly to the generation of CAM due to their high correlations and redundancies (see Fig. 1d). Meanwhile, the most informative activation maps should be retained to ensure that the visual explanations generated are as accurate as possible. Accordingly, a simple but effective unsupervised dimension reduction is proposed using KL-divergence loss between each activation map and all other maps, defined as

$$D_{\text{KL}}^c = \text{KL}(\mathbb{U}^c \parallel \mathbb{U}^{c \setminus \{c\}}), \quad c \in [1, \dots, L \times C] \quad (1)$$

where the lower values correspond to redundant activation maps. In other words, it aims to select activation maps $\bar{\mathbb{U}} \in \mathbb{R}^{\bar{C} \times w \times h}$ that minimize information loss and ensure computation efficiency. Hence, the number of activation maps was experimentally reduced by a factor of two (i.e., $\bar{C} = 1/2(L \times C)$). Then, the selected activation maps with maximal KL-divergence loss will be normalized to serve as masks \mathbb{N} for the next phase.

B. Phase 2: Local Score Maps for Activation Maps

The first step in this phase is to mask the input image by applying the normalized activation maps as

$$\bar{X}^c = \mathbb{N}^c \circ X, \quad c = [1, \dots, \bar{C}] \quad (2)$$

where \circ indicates the Hadamard product. The masked images \bar{X} are then passed into the tree crown detector f to calculate the local score maps S . While the baseline Score-CAM (and its modified versions [5]–[7]) calculates a global score for each activation map, the proposed Crown-CAM provides a score map per activation map that is locally weighted based on the predicted bounding boxes and their confidence scores as

$$S_k^c = \text{IoU}(B_k^X, B_k^{\bar{X}^c}) + |Y_k^X - Y_k^{\bar{X}^c}|, \quad (3)$$

in which $B^{\bar{X}^c}$, $Y^{\bar{X}^c}$, and k are the predicted bounding boxes, their confidence scores, and index of predicted boxes, respectively. Accordingly, important areas of each score map are weighted using the IoU between the predicted bounding boxes derived from the input image and the activation-based image masks as well as the absolute difference between their confidence scores. To alleviate boundary effects of tree crown areas in the local score maps, 2D Gaussian kernels with $\bar{w}_k \times \bar{h}_k$ dimensions are fitted to the center of predicted tree crowns with variance σ^2 as

$$\mathbb{Z}_k^c(B_k^{\bar{X}^c}) = S_k^c \cdot \mathcal{N}(B|B_k^{\bar{X}^c}, \sigma^2) \quad (4)$$

Algorithm 1 Pseudo-code of Crown-CAM

INPUTS: Input image X , Detection model $f(\cdot)$, Feature layers $l \in [1, \dots, L]$, Desired number of channels \bar{C}

OUTPUT: Class activation map M_{CrownCAM}

NOTATIONS: Bounding boxes B , Confidence scores Y , Activation of layers \mathbb{A} , KL loss D_{KL} , IoU metric $\text{IoU}(\cdot, \cdot)$, Local score maps S , Gaussian-fitted score maps Δ , Activation and local score maps after channel suppression $\bar{\mathbb{U}}$ and $\bar{\mathbb{Z}}$

```

 $B^X, Y^X, \mathbb{A}_\ell \leftarrow f(X)$  ▷ Apply model to image
for  $\ell$  in  $[1, \dots, L]$  do
    for  $c$  in  $[1, \dots, C]$  do
         $\mathbb{U}_\ell^c \leftarrow \text{Up-sample } \mathbb{A}_\ell^c$ 
    end
end
for  $c$  in  $[1, \dots, L \times C]$  do
     $D_{\text{KL}}^c = \text{KL}(\mathbb{U}^c \parallel \mathbb{U}^{c \setminus \{c\}})$  ▷ Unsupervised loss
end
 $\bar{\mathbb{U}} \leftarrow \text{Select } \bar{C} \text{ indices of } \mathbb{U} \text{ with maximal } D_{\text{KL}}$ 
for  $c$  in  $[1, \dots, \bar{C}]$  do
     $\mathbb{N}^c \leftarrow \text{Normalize } \bar{\mathbb{U}}^c$ 
     $\bar{X}^c \leftarrow \mathbb{N}^c \circ X$  ▷ Hadamard product
     $B^{\bar{X}^c}, Y^{\bar{X}^c} \leftarrow f(\bar{X}^c)$  ▷ Apply model to masked images
    for  $k$  in  $[1, \dots, \text{length}(Y^{\bar{X}^c})]$  do
         $S_k^c = \text{IoU}(B_k^X, B_k^{\bar{X}^c}) + |Y_k^X - Y_k^{\bar{X}^c}|$  ▷ Score maps
         $\mathbb{Z}_k^c(B_k^{\bar{X}^c}) = S_k^c \cdot \mathcal{N}(B|B_k^{\bar{X}^c}, \sigma^2)$  ▷ Fit Gaussians
    end
    Suppress  $\mathbb{Z}^c, \bar{\mathbb{U}}^c$  iff  $\sum_{\kappa} \mathbb{Z}_{\kappa}^c = 0$ 
end
 $\Delta^c \leftarrow \frac{\exp(\hat{\mathbb{Z}}^c)}{\sum_{c=1}^{\bar{C}} \exp(\hat{\mathbb{Z}}^c)}, \sum_c \Delta^c = 1$  ▷ Scores to probabilities
 $M_{\text{CrownCAM}} \leftarrow \text{ReLU}(\sum_c \Delta_c \cdot \hat{\mathbb{U}}_c)$ 

```

where $\mathbb{Z} \in \mathbb{R}^{\bar{C} \times w \times h}$ and \mathbb{N} are zero maps and 2D Gaussian function, respectively.

The baseline Score-CAM and its modified versions apply softmax (i.e., $\exp(\rho)/\sum_{\delta} \exp(\rho)$) to the global score vector of activation maps to ensure that the sum of values is one (i.e., probability interpretation). However, background channels may adversely affect the generation of CAMs in these methods. Here is a simple example that clarifies the issue with a score vector of length 10. If no object of interest is present in the input image, then all elements in Score-CAM's score vector will be zero. However, applying softmax to the zero vector will result in 0.1 per its elements. In other words, the CAM will be generated based on the weighted sum of all activation maps with non-zero factors of 0.1, thus allowing non-target-related areas to be activated (see the bottom row of Fig. 1b). To address this problem, the proposed Crown-CAM suppresses background channels if all elements of local score maps are zero. Thus, it minimizes the impact of false background regions on the final generated CAM (see the bottom row of Fig. 1c). Finally, the softmax is applied on the remaining local score maps (i.e., $\hat{\mathbb{Z}}$) and the final CAM is obtained by

$$M_{\text{CrownCAM}} = \text{ReLU}(\sum_c \Delta_c \cdot \hat{\mathbb{U}}_c) \quad (5)$$

where Δ represents softmax-applied local score maps and ReLU is used to remove activations with negative effects.

III. PROPOSED LOCALIZATION METRICS

For the classification task, CAMs are evaluated by either the percentage drop (or increase) in the model's score when CAM is provided as input (i.e., Drop (or Increase) in Confidence metrics) or the number of times the Drop-in-Confidence metric is less for one method than in another (i.e., Win metric). However, these metrics do not exploit the contextual information in a scene and therefore fail to deal with the challenges involved in tree crown detection. Moreover, for the WSL setting, the object localization is calculated based on a labeled bounding box and a rectangle drawn around the largest segment of interest. However, it has not been extended to dense object detection, cannot evaluate the inaccuracy of generated CAMs without objects of interest, and cannot quantify dense boxes simultaneously. To address these limitations, we introduce two IoU-based metrics, $\text{CAMIoU}^{\text{FG}}$ and $\text{CAMIoU}^{\text{BG}}$, which indicate the accuracy of CAMs in detecting tree crowns and avoiding background regions. These metrics are calculated by generating three masks based on the CAM and bounding boxes of the tree crowns as

$$\text{Mask}^{\text{CAM}} = \begin{cases} 1, & \text{if } \text{CAM}(i, j) \geq \text{Threshold} \\ 0, & \text{otherwise} \end{cases} \quad (6)$$

$$\text{Mask}^{\text{FG (or BG)}} = \begin{cases} 1 \text{ (or } 0), & \text{if } \zeta(i, j) \in \mathbb{B}^X \\ 0 \text{ (or } 1), & \text{otherwise} \end{cases} \quad (7)$$

where $\zeta \in \mathbb{R}^{w \times h}$ and \mathbb{B}^X refer to a zeros (or ones) map with spatial locations of (i, j) and ground-truth tree crown bounding boxes of the input image, respectively. Then, the localization metrics can be defined as follows.

$$\text{CAMIoU}^{\text{FG}} = \frac{\text{Mask}^{\text{CAM}} \cdot \text{Mask}^{\text{FG}}}{\text{Mask}^{\text{CAM}} + \text{Mask}^{\text{FG}}} \quad (8)$$

$$\text{CAMIoU}^{\text{BG}} = \frac{\text{Mask}^{\text{CAM}} \cdot \text{Mask}^{\text{BG}}}{\text{Mask}^{\text{CAM}} + \text{Mask}^{\text{BG}}} \quad (9)$$

In summary, the numerators represent the overlap areas between the important areas of CAM and tree crowns or backgrounds, while the denominators indicate their union areas. Therefore, the most reliable approaches must focus on tree crown regions (i.e., higher $\text{CAMIoU}^{\text{FG}}$) while avoiding background distractors (i.e., lower $\text{CAMIoU}^{\text{BG}}$).

IV. EMPIRICAL EVALUATIONS

In this section, the effectiveness of the proposed Crown-CAM is evaluated using the public NEON tree crown dataset [10]. This dataset provides 10000 hand-labelled tree crowns from six forests across the U.S.A representing a variety of landforms, vegetation, climates, and ecosystem dynamics. To perform evaluations, three crown detectors with ResNet-50 backbone including pre-trained DeepForest (i.e., RetinaNet) [3], Faster-RCNN [11], and Cascade-RCNN [12] were used. The backbone features of the Faster-RCNN and Cascade-RCNN networks (implemented in Detectron2 [13]) were initialized with those from the pre-trained DeepForest model [3]. Following that, the networks were trained on NEON's training set for 80 epochs with mini-batches of size 16. The proposed Crown-CAM is compared with three gradient-free methods, namely the baseline Score-CAM [4], Augmented Score-CAM [7], and Eigen-CAM [9]. The Eigen-CAM [9] is a simple and efficient method for calculating the principle components of the learned convolutional activations, but it is not class-aware. In contrast, the Augmented Score-CAM [7] is a computationally expensive method that uses the geometric augmentations (i.e., rotation & translation) to generate CAMs from combined activation maps of multiple input images. All experiments were conducted on an Nvidia RTX 3090 with 24GB RAM. We use images with width (w) and height (h) of 400×400 , while other parameters are set to $L = 5$, $C = 256$, $\bar{C} = 640$, $\sigma^2 = 0.7$, and Threshold = 0.4.

For quantitative comparison, the performance of visual explanation methods is verified on the test set of the NEON dataset using two introduced localization metrics (i.e., (8) and (9)). Table I shows the average accuracy and average inaccuracy of visual explanations generated by different tree crown

TABLE I
QUANTITATIVE COMPARISON OF GRADIENT-FREE VISUAL EXPLANATION METHODS IN TERMS OF PROPOSED METRICS FOR TREE CROWN DETECTION.

Tree Crown Detector	Proposed Crown-CAM		Score-CAM [4]		Augmented Score-CAM [7]		Eigen-CAM [9]	
	$\text{CAMIoU}^{\text{FG}} (\uparrow)$	$\text{CAMIoU}^{\text{BG}} (\downarrow)$	$\text{CAMIoU}^{\text{FG}} (\uparrow)$	$\text{CAMIoU}^{\text{BG}} (\downarrow)$	$\text{CAMIoU}^{\text{FG}} (\uparrow)$	$\text{CAMIoU}^{\text{BG}} (\downarrow)$	$\text{CAMIoU}^{\text{FG}} (\uparrow)$	$\text{CAMIoU}^{\text{BG}} (\downarrow)$
DeepForest [3]	29.64	19.81	24.96	23.37	25.64	24.89	14.91	32.28
Faster-RCNN	26.13	25.10	21.72	34.98	23.41	31.26	5.26	34.60
Cascade-RCNN	42.47	6.18	25.44	2.72	33.06	4.79	12.80	0.77

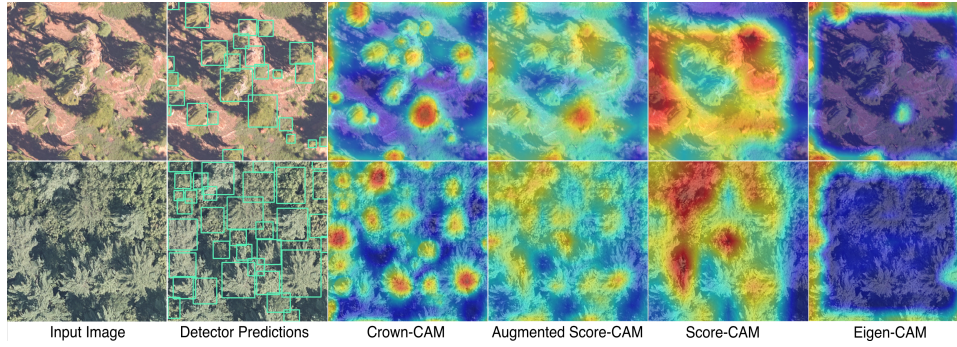


Fig. 3. Qualitative comparison of proposed Crown-CAM with gradient-free visual explanation methods including baseline Score-CAM [4], Augmented Score-CAM [7], and Eigen-CAM [9] for tree crown detection in aerial images. The visual explanations of proposed Crown-CAM are highly interpretable and helps to localize densely-distributed tree crowns at finer-grain level compared to existing methods.

detectors. Accordingly, the proposed Crown-CAM outperformed other post-hoc gradient-free methods with respect to the localization effectiveness of generated CAMs, while Eigen-CAM achieved the worst results due to its inherent limitations. Note that other methods in the case of using the Cascade-RCNN model have lower $\text{CAMIoU}^{\text{BG}}$ values due to their failure to generate salient regions that capture full tree crowns, thus resulting in lower intersections of generated CAMs with background regions. The proposed Crown-CAM achieves average improvements in $\text{CAMIoU}^{\text{FG}}$ (and $\text{CAMIoU}^{\text{BG}}$) metric up to 8.7, 5.3, and 21.7 (and 3.3, 9.8, and 16.5) compared to the baseline Score-CAM [4], Augmented Score-CAM [7], and Eigen-CAM [9], respectively. In addition, the CPU run-time for the Crown-CAM, Score-CAM, Augmented Score-CAM, and Eigen-CAM is 26.3, 18.4, 135.2, and 0.2 seconds per image, respectively. The results demonstrate the effectiveness of the proposed Crown-CAM in detecting tree crown areas while suppressing background regions in challenging detection scenarios involving an abundance of objects with different scales & viewpoints and background distractions.

Furthermore, the qualitative comparisons of visual explanations generated by different methods and the Cascade RCNN model are shown in Fig. 3. This figure illustrates two scenarios that include a mixture of tree crowns and background regions as well as densely structured forests. Based on the generated CAMs, the visual explanations of the proposed Crown-CAM are more reliable in detecting tree crown locations compared with other existing methods that overlap irrelevant areas or result in uncertain ambiguous regions. Additionally, Fig. 1d illustrates the ablation analysis for the proposed unsupervised dimension reduction, demonstrating its negligible impact on the generated CAM while reducing computational complexity.

V. CONCLUSION

In this paper, a novel reliable visual explanation method and two localization metrics for tree crown detection in aerial images were introduced. The proposed Crown-CAM exploits unsupervised dimension reduction of activation maps to efficiently calculate local score maps emphasizing tree crown areas while suppressing background regions. Additionally, two localization metrics were derived as a function of accurate and inaccurate CAMs. These are particularly effective for analyzing errors associated with false areas of an image highlighted

as salient and not carrying any contextual information about the expected tree crown detection. Empirical results of the proposed Crown-CAM demonstrated the great potential of exploring and developing reliable XAI methods for black-box tree crown detectors that can be intuitive to human understanding of interpretability.

ACKNOWLEDGMENTS

The authors would like to thank Mohammad Naser Sabet Jahromi from Aalborg University for reviewing this work and providing valuable comments and suggestions.

REFERENCES

- [1] A. Das and P. Rad, "Opportunities and challenges in explainable artificial intelligence (XAI): A survey," 2020. [Online]. Available: <https://arxiv.org/abs/2006.11371>
- [2] E. Tjoa and C. Guan, "A survey on explainable artificial intelligence (XAI): Toward medical XAI," *IEEE Trans. Neural Networks and Learning Systems*, vol. 32, no. 11, pp. 4793–4813, 2021.
- [3] B. G. Weinstein, S. Marconi, M. Aubry-Kientz, G. Vincent, H. Senyondo, and E. P. White, "DeepForest: A Python package for RGB deep learning tree crown delineation," *Methods in Ecology and Evolution*, vol. 11, no. 12, pp. 1743–1751, 2020.
- [4] H. Wang, Z. Wang, M. Du, F. Yang, Z. Zhang, S. Ding, P. Mardziel, and X. Hu, "Score-CAM: Score-weighted visual explanations for convolutional neural networks," in *Proc. CVPR Workshops*, 2020.
- [5] H. Wang, R. Naidu, J. Michael, and S. S. Kundu, "SS-CAM: Smoothed Score-CAM for sharper visual feature localization," 2020. [Online]. Available: <https://arxiv.org/abs/2006.14255>
- [6] R. Naidu, A. Ghosh, Y. Maurya, S. R. N. K., and S. S. Kundu, "IS-CAM: Integrated Score-CAM for axiomatic-based explanations," 2020. [Online]. Available: <https://arxiv.org/abs/2010.03023>
- [7] R. Ibrahim and M. O. Shafiq, "Augmented Score-CAM: High resolution visual interpretations for deep neural networks," *Knowledge-Based Systems*, vol. 252, p. 109287, 2022.
- [8] R. R. Selvaraju, M. Cogswell, A. Das, R. Vedantam, D. Parikh, and D. Batra, "Grad-CAM: Visual explanations from deep networks via gradient-based localization," *IJCV*, vol. 128, no. 2, pp. 336–359, 2020.
- [9] M. Bany Muhammad and M. Yeasin, "Eigen-CAM: Visual explanations for deep convolutional neural networks," *SN Computer Science*, vol. 2, no. 1, p. 47, 2021.
- [10] B. G. Weinstein, S. Marconi, S. A. Bohlman, A. Zare, A. Singh, S. J. Graves, and E. P. White, "A remote sensing derived data set of 100 million individual tree crowns for the National Ecological Observatory Network," *eLife*, vol. 10, 2021.
- [11] S. Ren, K. He, R. Girshick, and J. Sun, "Faster R-CNN: Towards real-time object detection with region proposal networks," in *Proc. NIPS*, C. Cortes, N. Lawrence, D. Lee, M. Sugiyama, and R. Garnett, Eds., vol. 28, 2015.
- [12] Z. Cai and N. Vasconcelos, "Cascade R-CNN: Delving into high quality object detection," in *Proc. CVPR*, 2018.
- [13] Y. Wu, A. Kirillov, F. Massa, W.-Y. Lo, and R. Girshick, "Detectron2," <https://github.com/facebookresearch/detectron2>, 2019.